

# Lorenz's Three Variable Model

Nick Mitchell

December 4, 2015

## Abstract

Lorenz's three variable model is briefly explained and examined in depth for three particular solution sets, varying one parameter. The complexity of the sets was found to increase with the varying parameter. The first set was shown to have one fixed point and non-chaotic motion, the second set was shown to have two attractors with non-chaotic motion, and the third set was found to have two chaotic attractors. All three sets exhibited almost identical behavior initially for extreme initial values.

## 1 Introduction

The term *chaos* has recently been used across many fields ranging from pure mathematics to biology to electrical engineering. Whether discussing the population of a certain species, the behavior of particular celestial bodies in orbit, or the growth patterns of plants, chaos has greatly improved our understanding of the world around us. While the applications have been fruitful and diverse, the initial discovery of chaos is rather serendipitous. In 1963 Edward N Lorenz published an article in the lesser known Journal of the Atmospheric Sciences proposing the idea of solutions for a particular system of differential equations that “vary in an irregular, seemingly haphazard manner, and, even when observed for long periods of time, do not appear to repeat their previous history” (Lorenz 1963). Despite being an entirely new declaration at the time, the matter has been studied by the likes of many over the past five decades. Resultantly, the potential solution sets to the system studied by Lorenz will be observed in more detail.

## 2 The Lorenz Equations

Lorenz began his study of chaos unknowingly through the study of certain hydrodynamical systems. He uses Rayleigh's (1916) studies of fluid flow for a system of uniform depth with a constant temperature difference between the upper and lower boundary surfaces. There is an obvious solution to this system, where there is no flow and the temperature is linearly proportional to the depth. However, should this

solution be unstable, convection will eventually result. Figure 1 provides a rough portrayal of the instability of Rayleigh’s steady state solution. From here, Lorenz then considers the case where motion is restricted to the x-z-plane. The governing equations of Saltzman (1962) are now applicable, along with the set of ordinary differential equations he derived. Lorenz then truncates Saltzman’s solutions to three terms and non-dimensionalizes the system to achieve the now famous Lorenz equations:

$$\dot{X} = -\sigma X + \sigma Y \quad (1)$$

$$\dot{Y} = -XZ + rX - Y \quad (2)$$

$$\dot{Z} = XY - bZ \quad (3)$$

Thus, the Lorenz equations are a simplified system of three ordinary, nonlinear differential equations in three variables with three parameters.

The variables of the Lorenz equations  $X$ ,  $Y$ , and  $Z$  denote varying properties of the fluid of interest.  $X$  is proportional to the intensity of the convective motion,  $Y$  is proportional to the temperature difference between ascending and descending currents, and  $Z$  is proportional to the distortion of the vertical temperature profile from linearity. Since Lorenz non-dimensionalized Saltzman’s solutions, each variable is a function of the dimensionless time. We will let  $t$  be dimensionless time and thus the dot notation ( $\dot{\phantom{x}}$ ) denotes differentiation with respect to  $t$ . These variables will be visualized from here on by three dimensional Cartesian coordinates, under the understanding that they do not represent spacial dimensions in Lorenz’s definition.

The parameters of the Lorenz equations  $\sigma$  and  $r$  denote physical characteristics of the fluid of interest, while  $b$  is a multiplicative constant.  $\sigma = \frac{\eta}{\rho a}$  is the Prandtl number: the dimensionless ratio of viscosity $[\eta]$  to density $[\rho]$  by thermal diffusivity $[a]$  (Lide, 2009).  $r = R_a/R_c$  is the ratio of the Rayleigh number of the fluid to the critical value of the Rayleigh number, which determines if the heat transfer is through conduction or convection. Each of the three parameters is usually assumed positive.

### 3 Solution Sets

Since the Lorenz Equations depends on three parameters, classification of solutions is extremely complicated. Particular combinations of  $\sigma$ ,  $r$ , and  $b$  can have drastically different results. Such combinations will be referred to as solution sets, using spanning sets of the vector  $\vec{P} = (\sigma, r, b)$  to describe them. To keep things relatively simple we will observe the effect  $r$  has for specific fixed values of  $\sigma$  and  $b$ . The main solution sets here for  $\vec{P}$  will keep  $\sigma = 10$ , and  $b = \frac{8}{3}$  fixed. We will then observe the following intervals in  $r$ :  $(0, 1)$ ,  $(1, 13.926)$ , and  $28$ . The first set

observes one stable fixed point at the origin, while the second observes two stable fixed points off of the origin. The third set observes the chaotic Lorenz attractor. The decision of which sets to study, as well as the characteristics of each set were in part determined from Jianke Yang's article *Lorenz Equations with Other Parameter Values*. Figure 2 shows Yang's summary of the system's behavior.

## 4 A Single Fixed Point

The first solution set of interest is the set  $\{\vec{P} = (10, r, \frac{8}{3}) : r \in (0, 1)\}$ . To obtain a general idea of how this set behaves we will start by considering paths on the Z-axis, and then paths farther from the Z-axis. The value of  $r = 0.1$  will suffice to display the behavior of the solution set.

Figure 3 shows us that paths starting on the Z-axis, with initial conditions  $X(0) = Y(0) = 0, Z(0) = z$ , remain bound to the Z-axis, and converge to the origin. Figure 4 shows that paths starting just off of the Z-axis move as a helix about the Z-axis, again converging to the origin. Figure 5 shows us that paths starting far from the Z-axis follow a slightly damped helical motion about the X-axis towards the origin, but surpass it. The paths then oscillate about the z-y-plane in a damped manner, still in a helical motion. Finally, the paths switch to a helix about the Z-axis, where it converges to the origin.

Figures 3 to 5 also tell us that the origin is a stable fixed point since all solutions converge there.

We can easily show that this solution set is not chaotic. Plotting two trajectories with slightly different initial conditions shows that the paths do not diverge, as shown in Figure 6.

We can then conclude that this solution set has one fixed point at the origin and exhibits non-chaotic behavior.

## 5 Two Attractors

Our next set of interest is the set  $\{\vec{P} = (10, r, \frac{8}{3}) : r \in (1, 13.926)\}$ . We can again get a good overview of the set by starting from the Z-axis and observing behavior as we move away. The value of  $r = 13$  will accurately display the behavior of the set.

We can see that paths along the Z-axis still remain on the axis and converge to the origin. However, this is no longer a stable solution as paths slightly off the Z-axis do not converge to the origin as shown in Figure 7.

We can also see that paths off the Z-axis evolve to one of two attractors, each being a fixed point and off of the origin as shown in Figure 8.

For more extreme initial conditions, this solution set exhibits behavior very similar to the last set with the two helical motions. However instead of converging to the origin the paths again evolve to either of two attractors as shown in Figure 9.

A test for sensitivity to initial conditions shows us that similar starting points evolve in a similar manner as shown in Figure 10.

We can then conclude that paths in this solution set evolve to one of two attractors, both of which exhibit non-chaotic behavior. Paths starting on the Z-axis converge to the origin without leaving the Z-axis. Also, this set displays behavior similar to the last set for more extreme initial conditions until it approaches the origin.

## 6 The Lorenz Attractor

The previous two sections have covered the interval of  $r \in (0, 1) \cap (1, 13.926)$  displaying interesting, but non-chaotic behavior. Increasing  $r$  past 13.926 leads to some complicated motion, with the most peculiar occurring at  $r = 28$ . As such, we will observe the behavior of the set containing the single value  $\vec{P} = (10, 28, \frac{8}{3})$ . By again starting on the Z-axis, we see that paths along the Z-axis again converge to the origin and it is still unstable as shown in Figure 11.

Our set again appears to have two attractors, but the solution curves are no longer bound to one of them, nor do they appear to converge to either. Looking at a solution curve over drastically different time intervals makes this quite clear as shown in Figure 12.

For more extreme initial conditions, we again see a familiar helical pattern, tending to the system of attractors as shown in Figure 13.

We can conclude that for all paths off of the Z-axis, the system evolves to two attractors, which it orbits between infinitely. By observing the one-dimensional projections of a solution curve, we can roughly determine the periodicity of the solution as shown in Figure 14.

We can observe that there is no noticeable periodicity in the solutions. Knowing that this often implies chaos, we then test for sensitivity to initial conditions as shown in Figure 15.

The two paths shown above differ by only  $(\Delta X, \Delta Y, \Delta Z, ) = (0.01, 0.01, 0.01)$  but follow completely independent paths after a significant period of time. We can then conclude that the system is sensitive to initial conditions. Since there is also no apparent repetition of the solutions, we can guess that the motion is chaotic.

## 7 Chaos

Bifurcation diagrams can be used to show whether a system is chaotic or not. These diagrams plot the long term periodic position of a path over varying characteristic parameter values. In our case we will plot the values of  $X(t)$  after a significant time for initial values around  $(X(0), Y(0), Z(0)) = (0, 0, 0)$  for different  $r$  values.

To construct a bifurcation diagram for the Lorenz system we approximate our differentials as very small changes, ie  $dx \simeq \Delta x$ . Thus for an equation  $\frac{dX}{dt} = F(X, Y, Z)$ , we can write  $\Delta X = F(X, Y, Z)\Delta t$ . We then state  $X_{k+1} = X_k + \Delta X$ , giving us our approximate iterative equations. Using Maple, we can plot a rough bifurcation diagram for the Lorenz system using very small  $\Delta t$  values as shown in Figure 16

Due to the restrictions in Maple, the bifurcation diagram only includes a few initial conditions. As a result the Bifurcation points are mostly lost. However we can guess that there is a bifurcation point at  $r = 1$  and another just before  $r = 14$  due to the jumps in the graph. This corresponds to the claims made by Yang stated earlier (Section 3). Yang also states that motion after  $r = 24.74$  will be chaotic, with unstable fixed points. This corresponds to our findings as shown in Figure 17.

Regardless of Maple's restrictions we can clearly see that there will eventually be chaotic motion after some value of  $r$ . Since the interval  $r = 26...30$  displayed on the right most image is purely chaotic motion, our previous  $r$  value of 28 did in fact result in chaos.

## 8 Conclusion

Lorenz's three variable model has many interesting characteristics. Of the solution sets studied, which account for a tiny portion of the infinite parameter range, we were able to witness how one parameter influenced the system. Though fixing  $\sigma$  and  $b$ , we were able to see how small values of  $r$  affected our solutions.

Positive values of  $r < 1$  caused the solution to have one fixed point at the origin, and all solution curves far enough from the Z-axis spiraled inwards about the X-axis, until their axis of rotation changed to the Z-axis, leading them to eventually converged to the origin. This helical behavior was found to be a characteristic of the other two solution sets, however the attractors changed. For values of  $r$  between 1 and 13.926, it was found that the solution all evolved to one of two attractors, neither of which were located at the origin. For  $r = 28$  these attractors were no longer stable. All solutions traveled infinitely and chaotically between both attractors.

In Lorenz' initial article, he claims that the solution may be accurate for slightly supercritical fluids. This means that for  $r$ -values less than or slightly more than one, the solutions may be accurate. For our solution sets, the only chaos was observed for  $r = 28$ , far beyond the realistic range. This means that as far as application is concerned, the chaotic behavior observed is irrelevant. However, Lorenz's observations are far more significant than the realistic application of the three variable model. His simplified model has been applied to many other systems including but not limited to those involving lasers, dynamos, circuits, chemical reactions, and osmosis. Thanks to him, the door to the study of chaos was opened, and a bountiful field has emerged.

## 9 References

- León, H. C. (2010, November 9). *Rayleigh Benard Convection* Retrieved from [https://www.youtube.com/watch?v=BbWWLbUee\\_8](https://www.youtube.com/watch?v=BbWWLbUee_8)
- Lide, David R., ed., *CRC Handbook of Chemistry and Physics, 89th Edition* (Internet Version 2009),  
CRC Press/Taylor and Francis, Boca Raton, FL
- Lorenz, E. N. (1963). Deterministic Nonperiodic Flow. *Journal of Atmospheric Sciences*, 20(2), 130–141.
- Taylor, J. R. (2005). Nonlinear Mechanics and Chaos. In  
*Classical Mechanics* (pp. 457–520). University Science Books.
- Yang, J. X. (n.d.). *Lorenz Equations with Other Parameter Values*. Retrieved from  
<http://www.emba.uvm.edu/~jxyang/teaching/Math266notes14.pdf>
- Hilborn, R. C. (n.d.). A Model of Convecting Fluids: The Lorenz Model. In  
*Chaos and Nonlinear Dynamics* (pp. 27–37). Oxford University Press.

## 10 Figures

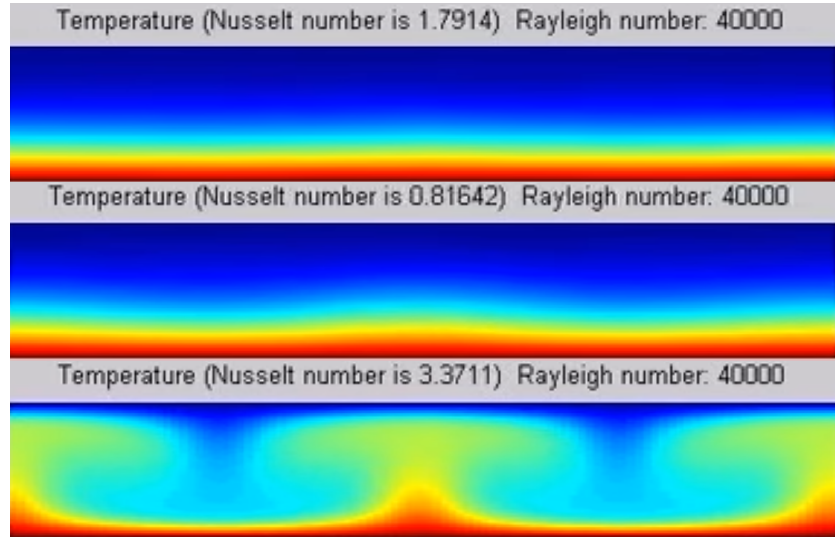


Figure 1: A visual display of the instability of Rayleigh's steady state solution. The first image displays a hypothetical tank filled with some fluid of uniform depth, with the temperature of the fluid being represented by the color, red being warmer than blue. The second image shows a perturbation from the solution that dramatically alters the temperature distribution in the third image: the definition of instability. (León, 2010)



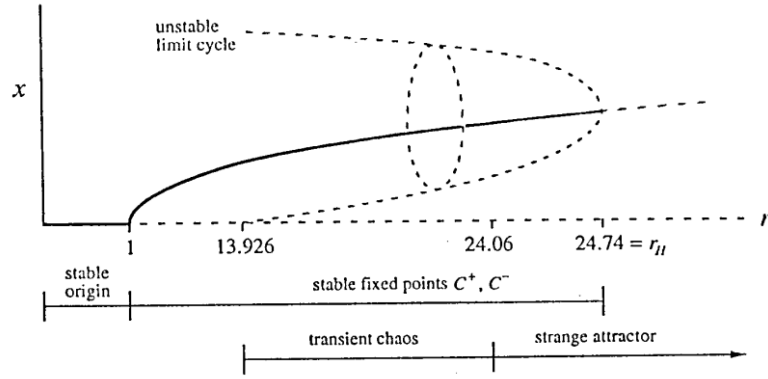


Figure 2: Summary of solution set behaviour for small  $r$  (Yang)

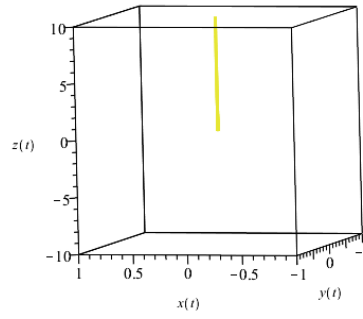


Figure 3: Initial conditions  $(X_0, Y_0, Z_0) = (0, 0, 10)$

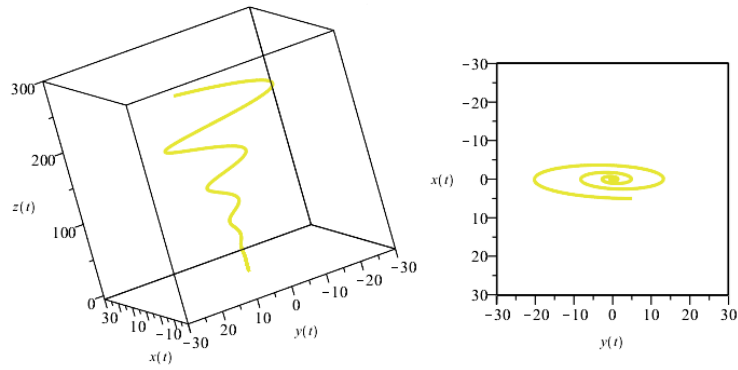


Figure 4: Initial conditions  $(X_0, Y_0, Z_0) = (5, 5, 250)$

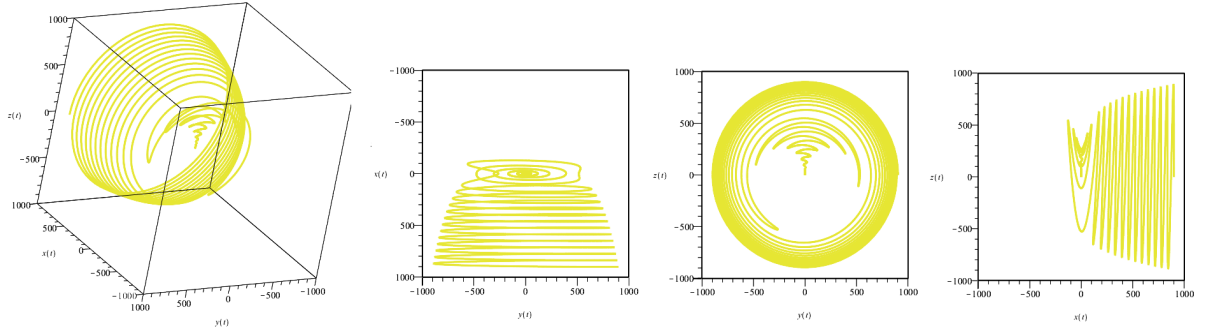


Figure 5: Initial conditions  $(X_0, Y_0, Z_0) = (900, 900, 0)$

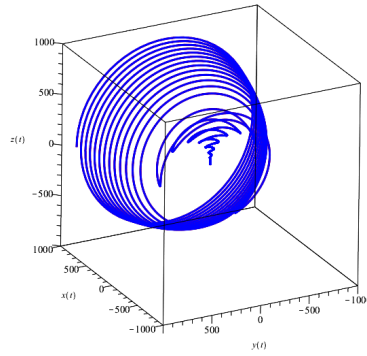


Figure 6: Initial conditions  $(X_0, Y_0, Z_0) = \{(900, 900, 0)[red], (900.1, 900.1, 0)[blue]\}$ . The red plot is not even visible as it is nearly identical to the blue plot.

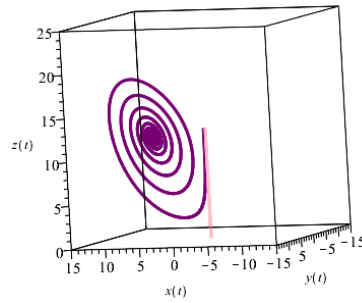


Figure 7: Initial conditions  $(X_0, Y_0, Z_0) = \{(0, 0, 12.5)[pink], (0.2, 0.2, 12.5)[purple]\}$ .

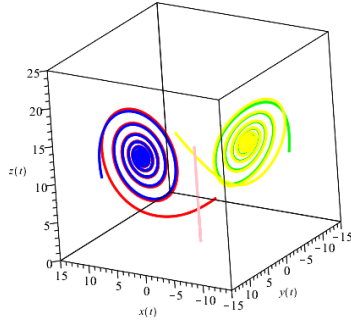


Figure 8: Initial conditions  $(X_0, Y_0, Z_0) = \{(-10, 10, 10)[red], (10, 10, 10)[blue], (-10, -10, 10)[green], (10, -10, 10)[yellow], (0, 0, 10)[pink]\}$ .

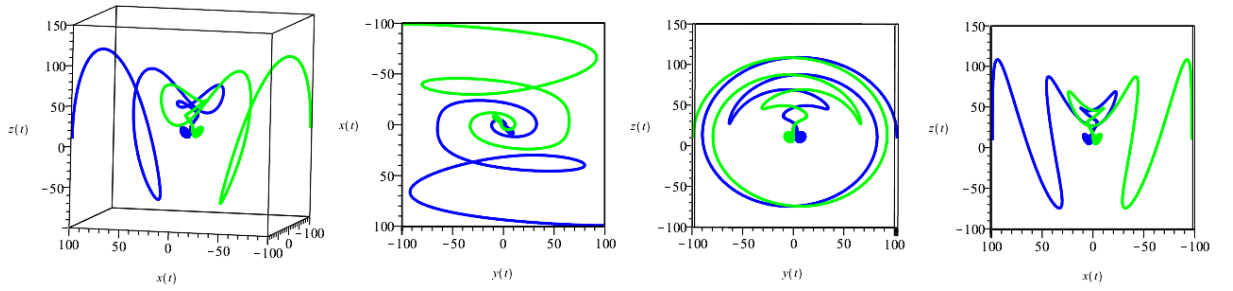


Figure 9: Initial conditions  $(X_0, Y_0, Z_0) = \{(99, 99, 10)[blue], (-99, -99, 10)[green]\}$ . These solutions bear striking resemblance to Figure 5.

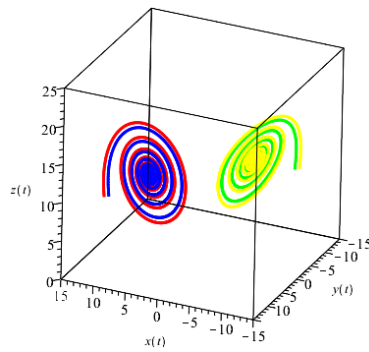


Figure 10: Initial conditions  $(X_0, Y_0, Z_0) = \{(10.5, 10.5, 10)[red], (10, 10, 10)[blue], (-10, -10, 10)[green], (-10.5, -10.5, 10)[yellow]\}$

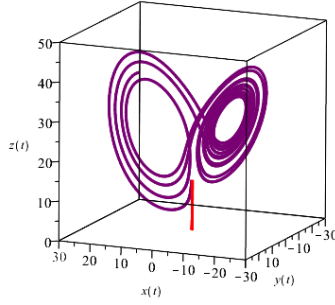


Figure 11: Initial conditions  $(X_0, Y_0, Z_0) = \{(0, 0, 12.5)[red], (0.2, 0.2, 12.5)[purple]\}$

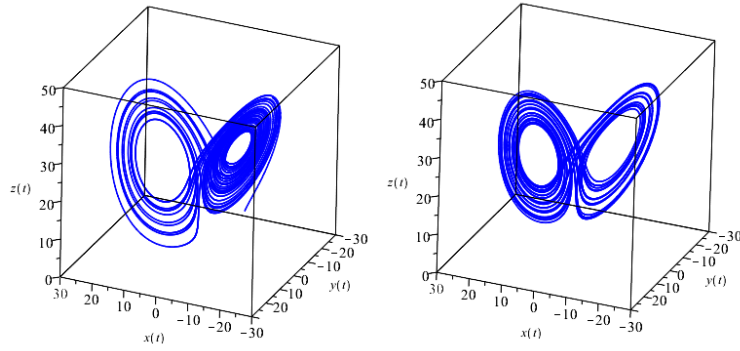


Figure 12: Initial conditions  $(X_0, Y_0, Z_0) = (-10, -10, 10)$ , over time intervals  $t = 0...30$  on the left, and  $t = 1000...1030$  on the right

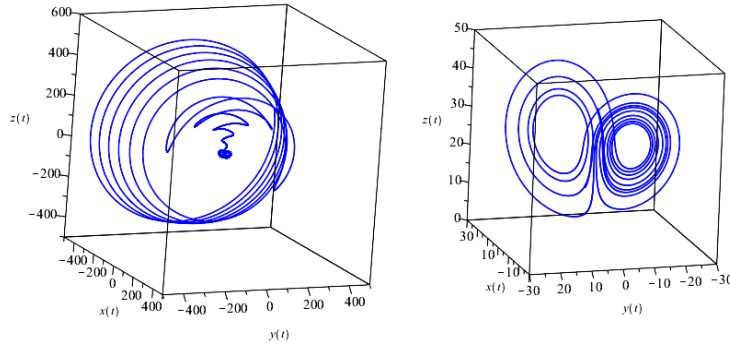


Figure 13: Initial conditions  $(X_0, Y_0, Z_0) = (-450, 450, 100)$ , over time intervals  $t = 0...30$  on the left, and  $t = 30...40$  on the right

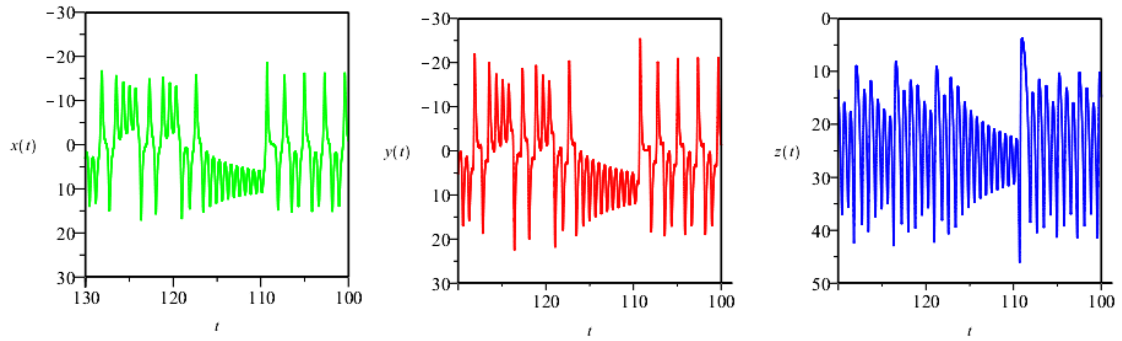


Figure 14: Initial conditions  $(X_0, Y_0, Z_0) = (10, 10, 10)$ , over the time interval  $t = 100 \dots 130$  is plotted, displaying the X-values[green], Y-values[red], and Z-values[blue] over time.

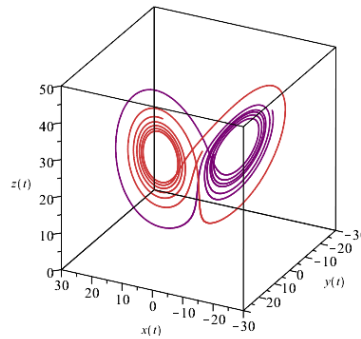


Figure 15: Initial conditions  $(X_0, Y_0, Z_0) = \{(10, 10, 10)[orange], (10.01, 10.01, 10.01)[purple]\}$ , over the time interval  $t = 400 \dots 405$  is plotted.

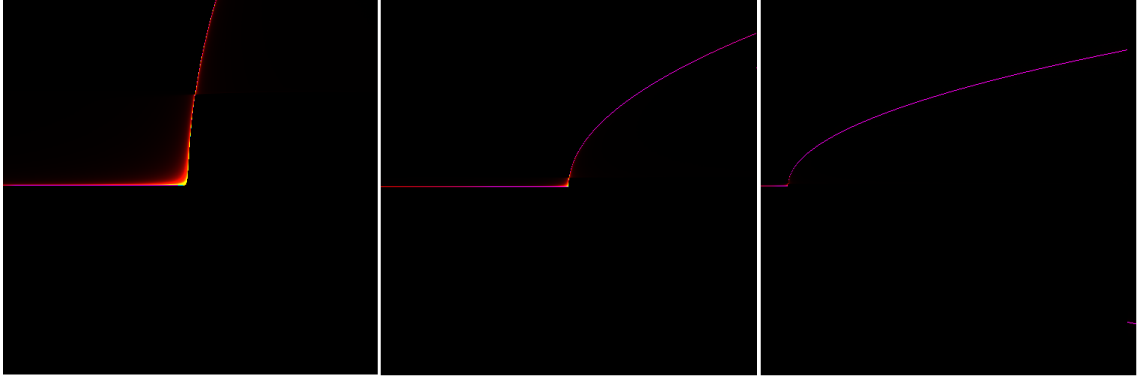


Figure 16: Initial conditions  $(X_0, Y_0, Z_0) = (10, 10, 10)$  are plotted in bifurcation diagrams over the following intervals in  $r$  :  $(0.9, 1.1)$ [*left*],  $(0, 2)$ [*middle*],  $(0, 14)$ [*right*]. The vertical axis represents  $X$  values ranging from -30 to 30.

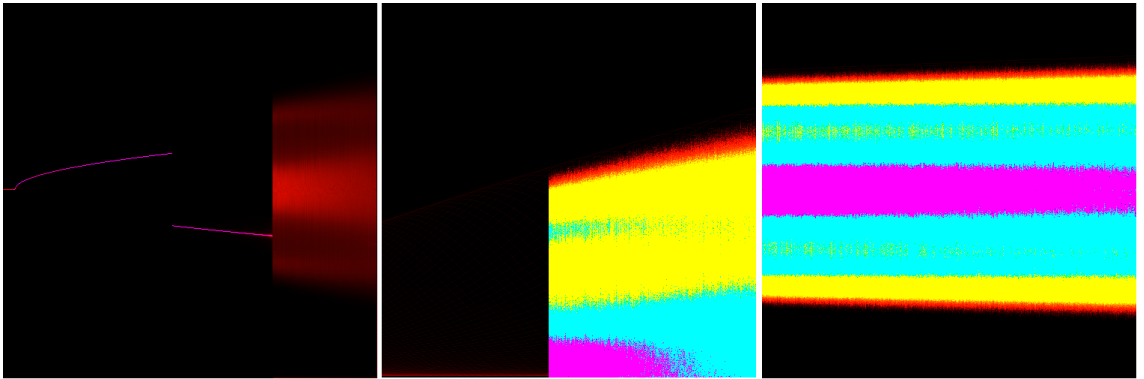


Figure 17: Initial conditions  $(X_0, Y_0, Z_0) = (10, 10, 10)$  are plotted in bifurcation diagrams over the following intervals in  $r$  :  $(0, 30)$ [*left*],  $(15, 30)$ [*middle*],  $(26, 30)$ [*right*]. The vertical axis represents  $X$  values ranging from -30 to 30.